Published March 30, 2009

Strabismus regulates asymmetric cell divisions and cell fate determination in the mouse brain

Blue B. Lake and Sergei Y. Sokol

Department of Developmental and Regenerative Biology, Mount Sinai School of Medicine, New York, NY 10029

The planar cell polarity (PCP) pathway organizes the cytoskeleton and polarizes cells within embryonic tissue. We investigate the relationship between PCP signaling and cell fate determination during asymmetric division of neural progenitors (NPs) in mouse embryos. The cortex of *Lp/Lp* (*Loop-tail*) mice deficient in the essential PCP mediator Vangl2, homologue of *Drosophila melanogaster* Strabismus (Stbm), revealed precocious differentiation of neural progenitors into early-born neurons at the expense of late-born neurons and glia. Although *Lp/Lp* NPs were easily maintained in vitro, they showed premature differentiation and loss of asymmetric distribution of Leu-Gly-Asn–enriched protein (LGN)/partner of inscuteable (Pins), a regulator of mitotic spindle orientation. Furthermore, we observed a decreased frequency in asymmetric distribution of the LGN target nuclear mitotic apparatus protein (NuMa) in *Lp/Lp* cortical progenitors in vivo. This was accompanied by an increase in the number of vertical cleavage planes typically associated with equal daughter cell identities. These findings suggest that Stbm/Vangl2 functions to maintain cortical progenitors and regulates mitotic spindle orientation during asymmetric divisions in the vertebrate brain.

Introduction

The planar cell polarity (PCP) pathway maintains cell polarity in the plane of epithelial tissues in *Drosophila melanogaster* embryos through the complex interplay of several core molecular components, including Frizzled, Dishevelled, Strabismus (Stbm), and Prickle (Tree et al., 2002). The same proteins also regulate polarized cell intercalation during gastrulation and neurulation in vertebrate embryos and polarization of inner ear cells in mammals (Sokol, 2000; Kibar et al., 2001; Jessen et al., 2002; Montcouquiol et al., 2003; Torban et al., 2004). In many cases, the PCP pathway has been proposed to modulate the cytoskeleton and influence cell morphology rather than cell fates (Wolff and Rubin, 1998). Nevertheless, some PCP components are essential for asymmetric cell division (ACD) of *Drosophila* sensory organ precursors (SOPs; Gho and Schweisguth, 1998; Bellaiche et al., 2004). Specifically, the transmembrane protein Stbm promotes the anterior cortical localization of partner of inscuteable (Pins), an activator of G protein signaling, which is required for proper orientation of the mitotic spindle and SOP daughter cell identity (Bellaiche et al., 2004). Although SOP divisions represent a highly specialized system, these observations suggest that the PCP pathway might influence cell fate determination during asymmetric division of other progenitor cells, as defined by unequal inheritance of fates between daughter cells and asymmetric distribution of specific proteins that may control this process. Given the potential importance of ACD in cell fate determination in the vertebrate brain, we investigated the possible involvement of PCP signals in regulating mammalian neurogenesis.

The development of the complex cytoarchitecture of the mammalian brain is thought to depend on the balance between symmetric and asymmetric divisions of neural progenitors (NPs) occupying the ventricular zone (VZ; Chenn and McConnell, 1995; Kosodo et al., 2004; Noctor et al., 2004; Gotz and Huttner, 2005). Vertical cleavage planes that are perpendicular to the ventricular surface usually result in symmetric divisions, whereas horizontally shifted cleavage planes may lead to asymmetry (Chenn and McConnell, 1995; Haydar et al., 2003; Kosodo et al., 2004; Gotz and Huttner, 2005). The latter were hypothesized to play a role in the specification of neuronal fates through

Correspondence to Sergei Y. Sokol: sergei.sokol@mssm.edu

Abbreviations used in this paper: ACD, asymmetric cell division; bFGF, basic FGF; GFAP, glial fibrillary acidic protein; NP, neural progenitor; NuMa, nuclear mitotic apparatus protein; PCP, planar cell polarity; Pins, partner of inscuteable; SOP, sensory organ precursor; Stbm, Strabismus; VZ, ventricular zone; XStbm, *Xenopus* Stbm.

Supplemental Material can be found at:
/content/suppl/2009/03/30/jcb.200807073.DC1.html
/content/suppl/2009/04/06/jcb.200807073.DC2.html

The Rockefeller University Press $30.00
J. Cell Biol. Vol. 185 No. 1 59–66
www.jcb.org/cgi/doi/10.1083/jcb.200807073

Published March 30, 2009

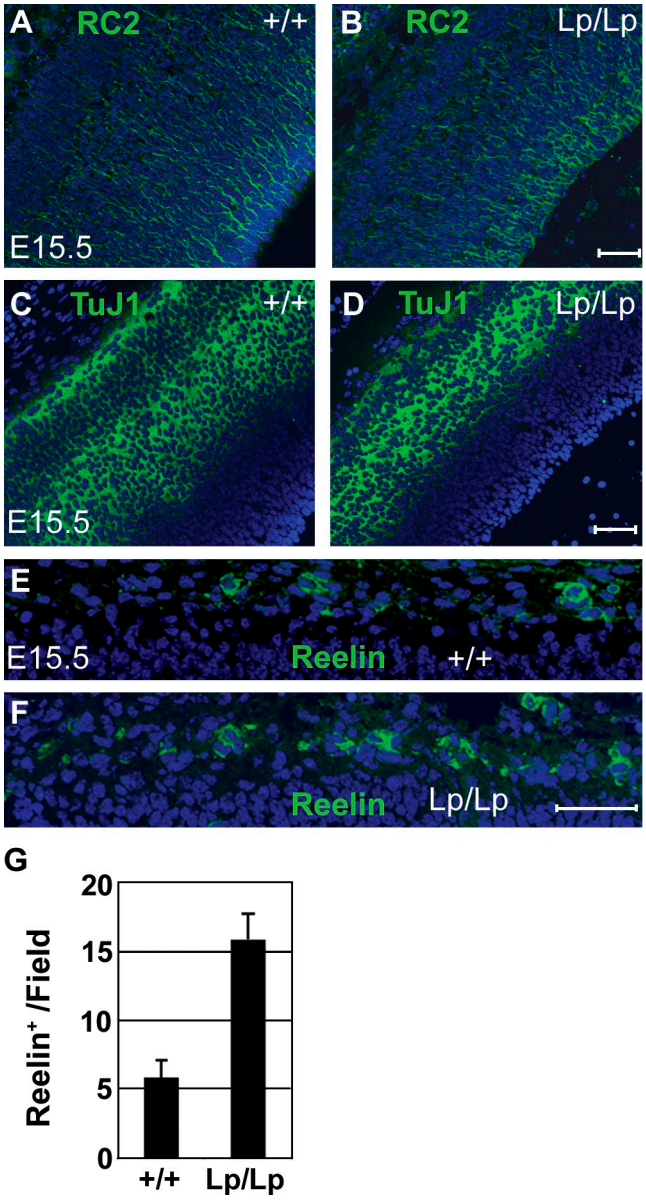

Figure 1. **Increased number of Reelin-positive neurons in E15.5 *Lp/Lp* cerebral cortices.** (A–F) Coronal sections of *Lp/Lp* or wild-type cortices (E15.5) were stained for RC2 (A and B), TuJ1 (C and D), Reelin (E and F, green), and DAPI (blue). (G) The number of Reelin-positive neurons is increased in three different *Lp/Lp* embryos (15.8 ± 1.9 per field, scored over four 110-µm-wide fields; F) as compared with wild-type mice (5.8 ± 1.3 per field; E). The total number of DAPI-positive nuclei in the marginal layer (scored over six 100-µm-wide fields per genotype) is 72.2 ± 7.4 for *Lp/Lp* and 61.2 ± 8.3 for wild-type littermates. Error bars indicate mean ± SD. Bars, 50 µm.

unequal inheritance of localized determinants (Betschinger and Knoblich, 2004; Gotz and Huttner, 2005). A disruption in the number of asymmetric divisions may deplete the progenitor population, leading to reduced brain size (Bond et al., 2002) and precocious neuronal differentiation (Sanada and Tsai, 2005). Therefore, factors regulating mitotic spindle orientation are expected to maintain the pool of NPs and regulate the sequential differentiation of cortical neurons and glia (Qian et al., 2000; Shen et al., 2006). Although a conserved Pins/G protein–dependent mechanism was found to regulate mitotic spindle orientation in

Table I. **Frequency of Reelin-positive cells in the E15.5 marginal zone**

Cell number	+/+	*Lp/Lp*
Reelin positive	5.8 ± 1.3	15.8 ± 1.9
DAPI positive	61.2 ± 8.3	72.2 ± 7.4

Reelin-positive cells were scored over four 110-µm fields per E15.5 embryo (+/+, *n* = 2; *Lp/Lp*, *n* = 3). DAPI-positive cells were determined over six 100-µm fields per genotype. The number of cells ± SD is given.

mammalian VZ progenitors (Sanada and Tsai, 2005; Konno et al., 2008), the involvement of PCP signals in this process has yet to be examined.

Results and discussion

To investigate a possible role of conserved PCP machinery in regulating vertebrate neurogenesis, we examined *Lp/Lp* (*Looptail*) mice that carry a point mutation in *Vangl2* (Kibar et al., 2001). This gene encodes a mammalian homologue of Stbm, a specific component of the PCP pathway in *Drosophila* (Wolff and Rubin, 1998; Montcouquiol et al., 2003). We constructed a mutated Stbm/Vangl2 cDNA carrying the *Lp/Lp* mutation that converts a serine to asparagine (S464N). The corresponding StbmS464N protein delocalized from the plasma membrane and failed to inhibit convergent extension movements in *Xenopus laevis* embryos, supporting the proposed loss of function phenotype of *Lp/Lp* mice (Fig. S1). Furthermore, although Vangl2 protein was broadly expressed in neuroepithelium of wild-type embryos, it was undetectable in *Lp/Lp* mice (Fig. S1, A–D), which is consistent with a previously reported loss of protein stability (Torban et al., 2007). Embryonic day (E) 15.5 cerebral cortices from *Lp/Lp* mice were relatively similar to those of *Lp/+* and +/+ mice in both gross morphology (Fig. S2) and a number of progenitors (RC2; Fig. 1, A and B) and revealed only a slight reduction in the neuronal layer (βIII-tubulin or TuJ1; Fig. 1, C and D). However, the number of Reelin-positive Cajal-Retzius cells, the earliest born neurons (Chae et al., 2004), was significantly increased in *Lp/Lp* cortices as compared with wild-type cortices (Fig. 1, E–G; and Table I). The total number of DAPI-positive nuclei in the marginal layer was largely unaffected, indicating that the increase is not caused by compaction of cells in the mutant cortex (Table I). These observations suggest precocious differentiation of *Lp/Lp* NPs into early-born neurons.

Premature differentiation of *Lp/Lp* NPs during corticogenesis would be expected to gradually diminish both the pool of progenitors and their derivatives: late-born neurons and glia. Consistent with this hypothesis, E18.5 cerebral cortices stained with hematoxylin/eosin and the TuJ1 antibody revealed a significant reduction in the overall size of the neocortex and a decrease of the neuronal population in *Lp/Lp* embryos as compared with *Lp/+* and wild-type embryos (Fig. 2, A and B). In the E18.5 *Lp/Lp* brain, we observed a reduction in glial fibrillary acidic protein (GFAP)–positive astrocytes and RC2-positive and Nestin-positive radial glia progenitors in *Lp/Lp* cortices as compared with *Lp/+* and wild-type cortices (Fig. 2, C, D, F, and G; and not

Published March 30, 2009

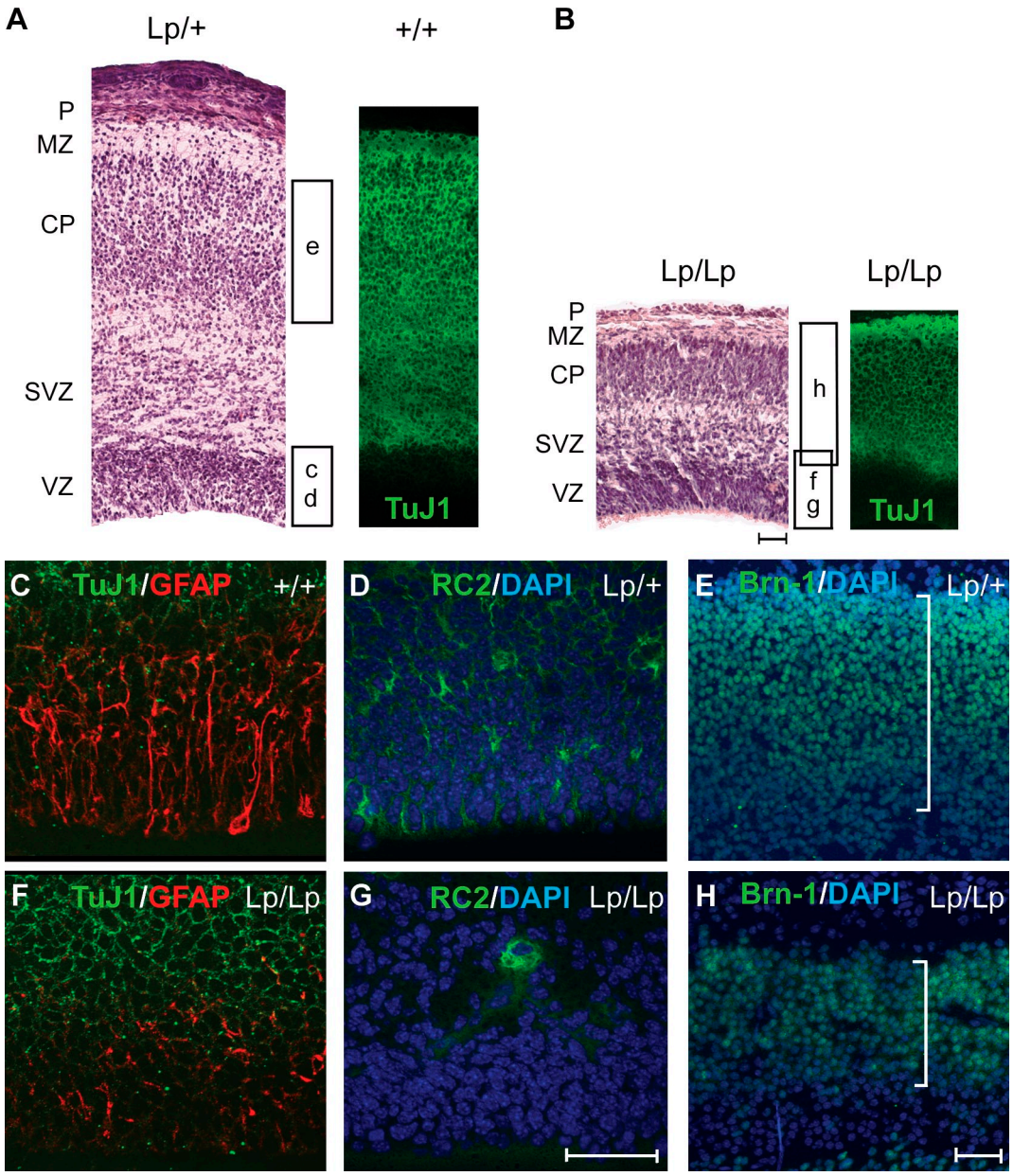

Figure 2. **Precocious differentiation of NPs in *Lp/Lp* mice.** (A–H) Coronal sections of *Lp/Lp* cortices at E18.5 are shown. They are reduced in size and show premature depletion of progenitors. Histological analysis of E18.5 neocortex, hematoxylin/eosin staining, and the corresponding TuJ1 staining (right) are shown for wild-type and *Lp/+* (A) and *Lp/Lp* (B) cortices. The respective positions of the pial layer (P), marginal zone (MZ; layer I), cortical plate (CP; layers II–VI), sub-VZ (SVZ), and VZ are shown. The corresponding regions examined in C–H are also shown. The astrocytes marked by GFAP (C and F), radial glia progenitors marked by RC2 (D and G), and late-born outer layer neurons marked by Brn-1 (E and H) were all significantly reduced in *Lp/Lp* mice. Brackets in E and H represent the relative size of the Brn-1 layer. Bars, 50 µm.

depicted). Late-born neurons marked by expression of Brn-1 (Chae et al., 2004) were also significantly decreased in *Lp/Lp* mice as compared with heterozygous littermates (Fig. 2, E and H), with a reduction detected as early as E15.5 (not depicted). Progressive reduction of the dividing progenitor population was further demonstrated after BrdU pulse labeling. When compared with heterozygous littermates, *Lp/Lp* cortices showed a similar number of dividing progenitors at E14.5 but a significant reduction by E17.5 (Fig. S2, A–F). The observed decrease in NP cells was not a result of increased apoptosis in *Lp/Lp* cortices, as we did not see a significant change in the number of cells with activated caspase 3 at both E14.5 and E17.5 (Fig. S2, G–J; and not depicted). Together, these findings suggest that *Lp/Lp* progenitors prematurely differentiate into early neuronal lineages at the expense of later born neurons and glia.

To study the intrinsic differentiation potential of *Lp/Lp* NPs, we established in vitro cultures and analyzed cell differentiation using conventional techniques (Chandran and Caldwell, 2004). NP cultures were derived from the developing cerebellum (E18.5) or cerebral cortex (E14.5) of *Lp/Lp* embryos as well as from *Lp/+* and +/+ littermates. When maintained as undifferentiated neurospheres in the presence of basic FGF (bFGF)

Published March 30, 2009

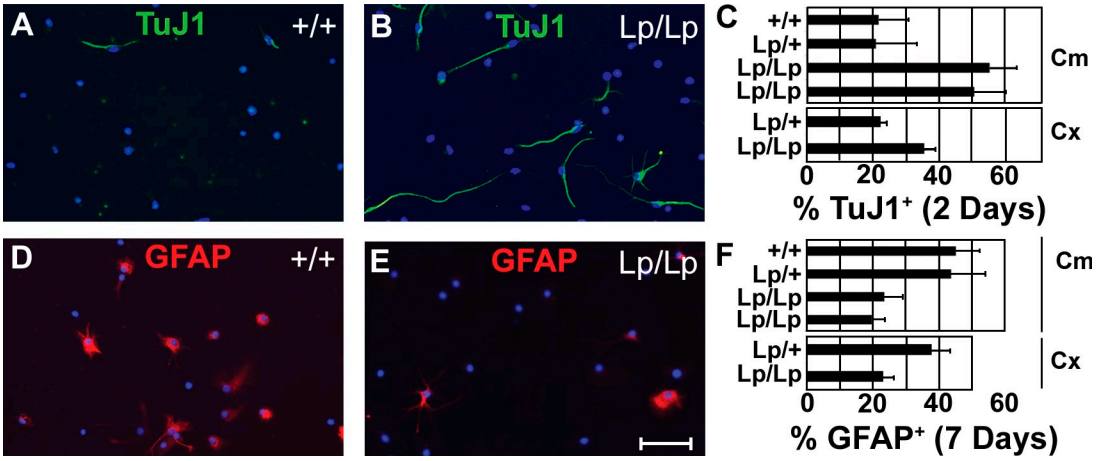

Figure 3. **Precocious differentiation of *Lp/Lp* NPs in vitro.** Progenitors derived from the E18.5 cerebellum (Cm) or E14.5 cortex (Cx) were obtained from *Lp/Lp* mice and compared with NPs obtained from *Lp/+* and/or +/+ littermates. Cerebellar progenitors were also obtained and compared between two different *Lp/Lp* mice. Dissociated cells were cultured in vitro under conditions that promote sequential neuronal then astrocytic differentiation. (A–C) In the absence of bFGF/EGF for 2 d, NPs formed TuJ1-positive neurons. (D–F) Addition of 2% serum to these cells at day 3 and culture for four additional days allowed astrocyte differentiation that was scored by GFAP staining. (A, B, D, and E) Images shown are for cerebellar progenitors. Frequencies of TuJ1⁺ (C) and GFAP⁺ (F) cells were scored per total number of DAPI-positive cells. Error bars indicate mean ± SD. Bar, 50 µm.

and EGF, all precursors showed similar expression levels of progenitor markers (Fig. S3 A), including *Nestin* and *Mash1* and the radial glia markers *BLBP* and *Glast* (Conti et al., 2005). All cell lines further showed a low expression level of *Dlx2*, a marker of transiently amplifying neuronal progenitors (Fig. S3), and did not express the neuronal marker TuJ1 or the astrocytic marker GFAP (not depicted). Furthermore, in the presence of bFGF and EGF, the NP lines grew as neurospheres at similar rates independent of the genotype, indicating that self-renewal was not affected by the mutation (Fig. S3 B). After withdrawal of bFGF and EGF from the medium, culturing under adherent conditions resulted in neuronal differentiation, with TuJ1-expressing neurons appearing after 2 d. A greater number of TuJ1-expressing neurons was observed for *Lp/Lp* NP cultures (Fig. 3, A–C). To determine the potential of these cultures to subsequently generate glial lineages, the culture medium was complemented with 2% FCS after 3 d of differentiation, and the number of astrocytes was determined after an additional 4 d in culture. *Lp/Lp* progenitors from both the cortex and the cerebellum produced significantly fewer astrocytes than *Lp/+* or wild-type progenitors (Fig. 3, D–F). These findings are consistent with the precocious differentiation observed in the *Lp/Lp* brain and suggest that *Vangl2* suppresses progenitor differentiation and promotes cell fate diversity.

One mechanism for suppressing premature overt differentiation is ACD that generates both a self-renewing progenitor and a committed precursor. Although our data are consistent with the idea that the PCP pathway regulates asymmetric divisions of vertebrate NP cells, the direct evidence supporting this hypothesis has been lacking. In *Drosophila* SOPs, Stbm activity was shown to maintain the asymmetric localization of Pins (Bellaiche et al., 2004), a regulator of G protein signaling, which is required for mitotic spindle orientation (Betschinger and Knoblich, 2004). A knockdown of a mouse homologue of Pins caused precocious differentiation of NPs both in vitro and in vivo (Sanada and Tsai, 2005), indicating its importance for proper spindle positioning in neural fate decisions. Furthermore, Leu-Gly-Asn–enriched protein (LGN), one of the two functionally conserved mammalian homologues of Pins (Du and Macara, 2004), is asymmetrically distributed in dividing NPs (Fuja et al., 2004). Thus, we decided to evaluate whether the PCP pathway influences mitotic spindle orientation in vertebrate NPs by monitoring subcellular localization of LGN during neuronal differentiation.

LGN localization was evaluated in cultures of dividing NPs isolated from wild-type, heterozygous, and mutant mouse embryonic brains after 24 h of differentiation in the bFGF/B27 medium (Fig. 4, A–F; Table II; Qian et al., 2000). Under these conditions, *Lp/Lp* NPs had a reduced number of mitoses after 3 d of culture as compared with *Lp/+* NPs (Fig. S3, C–E) but revealed increased TuJ1 expression consistent with enhanced neuronal differentiation (Fig. S3, F and C). Cultures were additionally treated with nocodazole to synchronize mitotic NPs for analysis of endogenous LGN asymmetry during each phase of the cell cycle. This permitted enrichment of mitotic progenitors without any apparent disruption in LGN distribution. Asymmetric LGN was detectable in a subcortical crescent in over a third of wild-type cells at prophase (Fig. 4, A–C) and prometaphase/metaphase, when it was found adjacent to the spindle poles (Fig. 4, D–F; and Table II). By anaphase, few asymmetries were visible (6.9% ± 3.3% of wild type), as LGN localized primarily to the cell center or midbody (n = 123; unpublished data). This indicates that spindle orientation is likely determined early within the cell cycle before separation of daughter chromosomes at anaphase. In two independent *Lp/Lp* cultures, the frequency of cells with asymmetrically distributed LGN was significantly decreased at both prophase and prometaphase/metaphase (Fig. 4, C and F; and Table II). These findings indicate that the Stbm/Vangl2 function in maintaining spindle orientation is conserved in neuronal precursors from *Drosophila* to mammals.

At the next stage of analysis, VZ cells were immunostained for the microtubule-binding nuclear mitotic apparatus

Published March 30, 2009

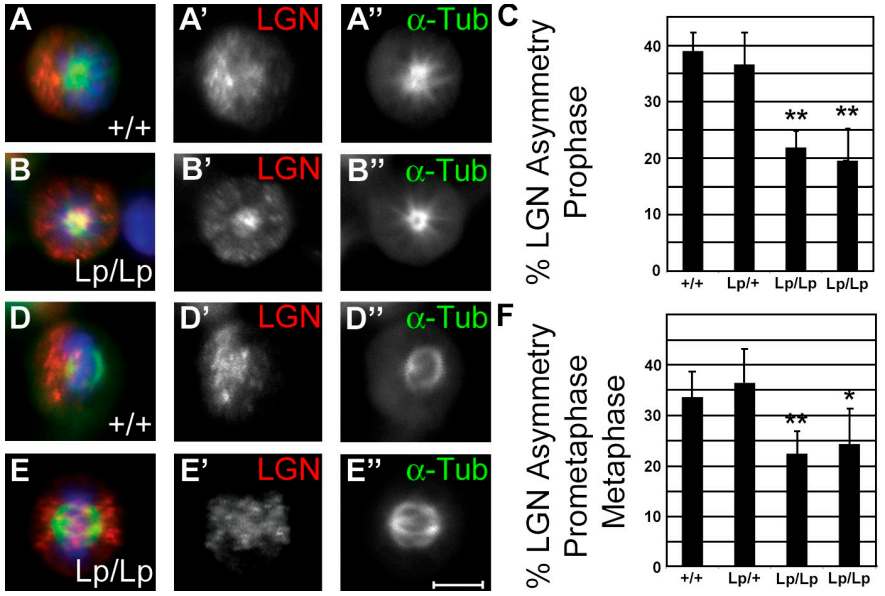

Figure 4. **Reduced number of asymmetric divisions in *Lp/Lp* progenitors.** NPs were allowed to differentiate for 24 h in the bFGF/B27 medium. (A, B, D, and E) 0.4 µg/ml nocodazole was added for the last 6.5 h and removed 0.5 h before cells were fixed and costained with antibodies against α-tubulin, LGN, and DAPI. Prophase (A and B) and prometaphase/metaphase (D and E) cells were identified by α-tubulin localization and exhibited either asymmetric (A–A″ and D–D″) or symmetric (B–B″ and E–E″) localization of LGN. The total number of cell divisions with LGN asymmetry (C and F) was scored at prophase (*Lp/Lp* embryo 1, $n = 257$; *Lp/Lp* embryo 2, $n = 294$; *Lp/+*, $n = 228$; +/+, $n = 207$) and prometaphase/metaphase (*Lp/Lp* embryo 1, $n = 416$; *Lp/Lp* embryo 2, $n = 445$; *Lp/+*, $n = 351$; +/+, $n = 331$). Statistical significance was determined against the *Lp/+* condition by a standard two-tailed Student's *t* test (*, $P < 0.05$; **, $P < 0.01$). Error bars indicate mean ± SD. Bar, 5 µm.

protein (NuMa), a putative target of LGN (Du and Macara, 2004) during ACD (Siller et al., 2006). NuMa is thought to determine spindle orientation between metaphase and anaphase by anchoring astral microtubules to the cell membrane. To maximize detection of asymmetric divisions that produce a progenitor cell and a neuron, we examined developing cortices at E14.5 near the peak in occurrence of this type of cell division (Haydar et al., 2003). Mitotic progenitors were identified in cortical sections by costaining for phosphohistone H3 (Fig. 5, A–G) and the centrosomal marker γ-tubulin. VZ progenitors showed increasing NuMa localization to the spindle poles during mitosis, with an asymmetric association apparent as early as prometaphase (Fig. 5 C). By late cytokinesis, centrosomes migrate to opposing poles in the close proximity to the cell membrane. At this point, NuMa staining may encompass both spindle and cortical domains consistent with its role in astral microtubule anchoring to the cell membrane. At metaphase/anaphase, the frequency of NuMa asymmetry at the spindle poles was significantly reduced in *Lp/Lp* mice (25.0%) as compared with heterozygotes (47.8%; Fig. 5, C–G). These observations support the hypothesis that Vangl2 is involved in promoting ACD during neuronal fate specification.

To directly assess whether asymmetric cleavage planes were disrupted in *Lp/Lp* mice, telophase cells were analyzed in E14.5 cortical sections costained with γ-tubulin and DAPI (Fig. 5, H–K). Cleavage orientation was defined by the angle between the line segregating daughter chromosomes and the ventricular surface (Chenn and McConnell, 1995). In prior studies, cleavage planes approaching 90° (vertical; Fig. 5 H) usually led to symmetric fates, whereas orientations closer to 0° (horizontal; Fig. 5 J) were more likely to be asymmetric, producing both a neuron and progenitor (Chenn and McConnell, 1995). We observed a significant increase in the number of vertical divisions (60–90°) in *Lp/Lp* mice as compared with heterozygous mice (Fig. 5 K and Table III). Because the greatest deviation occurred with divisions falling between 80–90° (*Lp/+*, 19.3% ± 3.9%; *Lp/Lp*, 32.7% ± 2.4%), this likely represents an increase in symmetrically dividing progenitors. The total number of divisions, indicated by BrdU incorporation (Fig. S2), remained unaffected at E14.5, which is consistent with Vangl2 regulating ACD of VZ progenitors rather than influencing cell proliferation in general. Additionally, E14.5 *Lp/Lp* cortices showed no significant changes in the apical distribution of ZO1, nonphosphorylated β-catenin, and atypical PKC (Fig. 5, A and B; not depicted; Gotz and Huttner, 2005). By late corticogenesis, BrdU incorporation and apical markers became significantly reduced in *Lp/Lp* mice (Fig. S2 and not depicted), which is consistent with a premature depletion of late-stage VZ progenitors. Together, our results support a role for Vangl2/Stbm in regulating mitotic spindle orientation and asymmetric progenitor divisions in the developing cortex.

These findings demonstrate the conservation of a molecular mechanism regulating ACD from fly to mouse embryos and provide the first evidence that the PCP pathway, commonly

Table II. **Frequency of LGN asymmetries in cerebellar NPs in vitro**

Cell cycle phase	Wild type	*Lp/+*	*Lp/Lp1*	*Lp/Lp2*
	%	%	%	%
Prophase	38.9 ± 3.4 ($n = 207$)	36.5 ± 5.8 ($n = 228$)	19.5 ± 5.7 ($n = 257$)	21.8 ± 2.9 ($n = 294$)
Prometaphase	33.6 ± 5.0 ($n = 331$)	36.3 ± 6.8 ($n = 351$)	24.3 ± 6.9 ($n = 416$)	22.3 ± 4.6 ($n = 445$)

Determined over four independent experiments. Percentage ± SD is given.

Published March 30, 2009

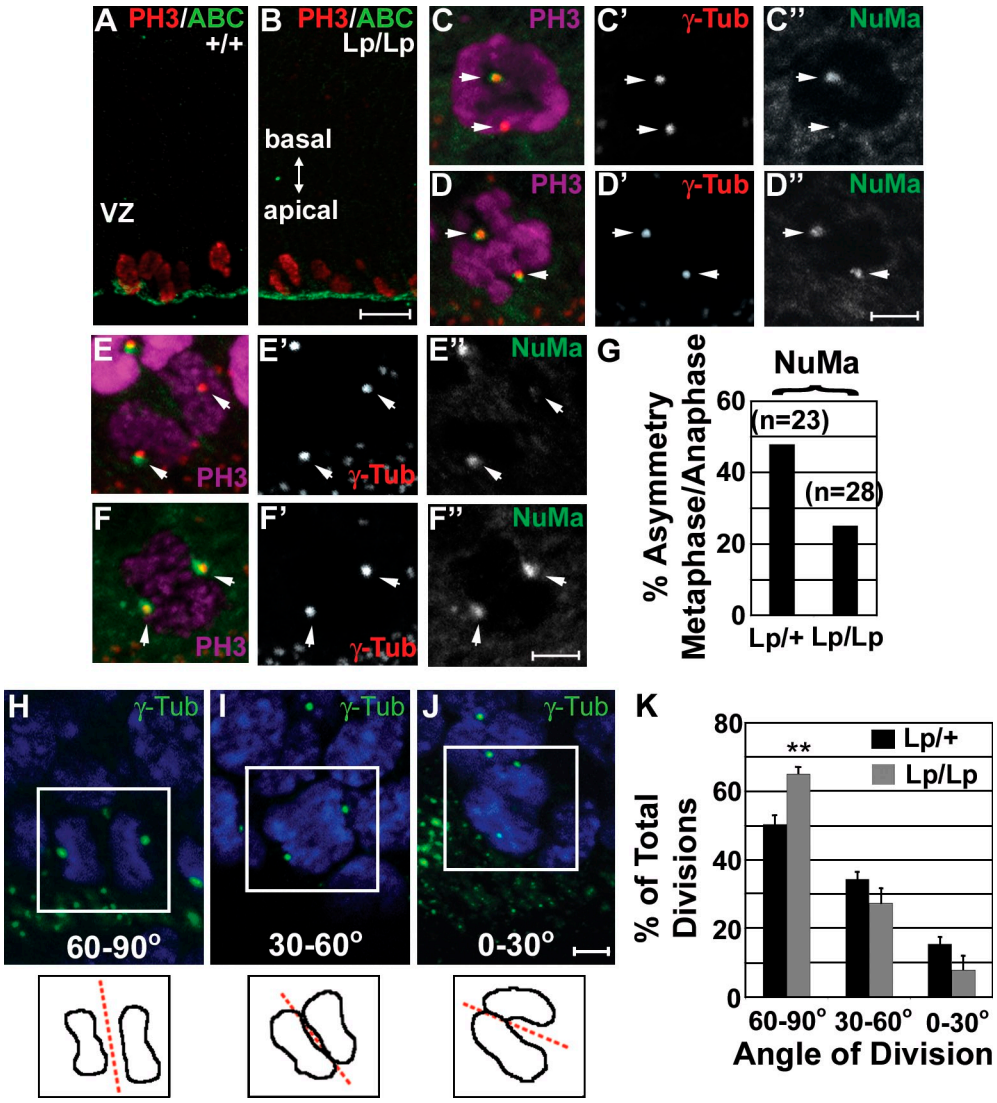

Figure 5. **Asymmetric divisions of NPs in the developing cortex.** (A and B) Coronal cryosections of E14.5 *Lp/Lp* ($n = 3$) and *Lp/+* ($n = 3$) forebrains were stained for phosphohistone H3 (PH3) to identify dividing VZ progenitors. Apical surfaces facing the lateral ventricle are indicated by nonphosphorylated (activated) β-catenin (ABC) staining. (C–F) Only cells adjacent to the lateral ventricle were analyzed and shown with their apical surfaces oriented down. Asymmetric (C–C″ and E–E″) and symmetric (D–D″ and F–F″) centrosomal localization of NuMa at prometaphase (C–D) and anaphase (E–F). Metaphase to anaphase NuMa asymmetries are summarized in G. Images shown are of *Lp/+* (C) and *Lp/Lp* (D–F) cortices. Arrows indicate centrosomes. (H–J) Cleavage plane orientation with respect to the apical surface was scored as described in Materials and methods and is presented in three broad categories: 60–90°, 30–60°, and 0–30°. Representative images are shown. Boxed regions indicate telophase nuclei represented graphically. (K) Comparison of cleavage plane orientation during anaphase/telophase of cortical cell divisions in *Lp/+* ($n = 172$) and *Lp/Lp* ($n = 112$) embryos (three for each genotype). Statistical significance was determined by a standard two-tailed Student's *t* test (**, $P < 0.01$). Error bars indicate mean ± SD. Bars: (B) 25 µm; (D″, F″, and J) 5 µm.

known to affect cell polarity and morphogenesis, plays a critical role in vertebrate neural fate decisions. Similar to what is observed in *Drosophila* SOP cells, Vangl2 may orient the mitotic spindle in a manner that promotes ACD (Bellaiche et al., 2004). Indeed, asymmetric cleavages within mouse cortical VZ progenitors must bypass apically positioned determinants (Chenn and McConnell, 1995; Kosodo et al., 2004; Lee et al., 2006), indicating the importance of mitotic spindle regulation in vertebrate neural fate decisions. This spindle control appears to depend on a conserved LGN–NuMa–Gαi complex, where subcortical LGN may anchor spindle poles to the cell membrane through coordinate interaction with both aster microtubule-associated NuMa and membrane-associated Gαi (Du and Macara, 2004). In murine VZ cortical progenitors, this complex may capture mitotic spindle poles symmetrically to promote similar daughter fates (Konno et al., 2008) or asymmetrically for cleavage planes that promote different daughter cell fates (Sanada and Tsai, 2005).

Consistent with a role in ACD, inhibition of G protein activity decreased asymmetric VZ cleavage planes and increased precocious neuronal differentiation in the mouse cortex (Sanada and Tsai, 2005). Similarly, in *Lp/Lp* embryos, the reduced asymmetry in distribution of LGN in vitro or NuMa in vivo was associated with precocious neuronal differentiation and depletion of the progenitor population. We propose that *Lp/Lp* NPs undergo an increased frequency of symmetric neurogenic

Published March 30, 2009

Table III. **Orientation of cleavage planes in VZ NPs in vivo**

Angle of division	*Lp/+* (*n* = 172)	*Lp/Lp* (*n* = 112)
	%	%
60–90°	50.3 ± 3.0	65.0 ± 2.2
30–60°	34.3 ± 2.5	27.3 ± 4.7
0–30°	15.5 ± 2.4	7.8 ± 4.4

Determined over three independent E14.5 mice per genotype. Percentage ± SD of total divisions is given.

divisions that normally occur during late stages of cortical development (Haydar et al., 2003). These results support a conserved role for Vangl2 in promoting ACD to preserve the pool of progenitors needed to complete multiple rounds of neurogenesis. Although it is likely that this function of Vangl2 is accomplished through its interactions with Dlg, LGN, and NuMa (Bellaiche et al., 2004; Du and Macara, 2004), this role may be permissive rather than instructive, as Vangl2 protein does not appear to be localized in embryonic brain cells at E12.5 (Fig. S1 B). Further studies are needed to identify direct molecular targets and upstream modulators of Vangl2 to understand the complex regulation of cell renewal and differentiation in the developing cortex.

Materials and methods

Mouse embryos

Lp/Lp mice of the *Lp/Lp*/Le stock were provided by D. Sassoon (Mount Sinai School of Medicine, New York, NY) and were maintained as described previously (Montcouquiol et al., 2003). For histology, E18.5 embryos (*Lp/Lp*, *n* = 4; *Lp/+*, *n* = 2) were fixed, embedded in paraffin, sectioned at 10–12 µm, and stained with hematoxylin/eosin.

NP culture

NPs were dissociated from E14.5 forebrain (cortical hemispheres) or E18.5 cerebella using 0.25% trypsin and/or gentle trituration. Single cells were seeded at a density of 10^5 cells/cm^2 in DME/F12 media containing N2 supplement (Johe et al., 1996), 10 ng/ml bFGF, 10 ng/ml EGF (Invitrogen), and 2% B27 supplement (Invitrogen). Neurospheres were passaged using Versene (Invitrogen) and/or gentle trituration and reseeded at a density of 1.25 × 10^4 cells/cm^2 without B27. All experiments were performed with NPs that were dissociated from passage 3–5 neurospheres.

Differentiation of dispersed NPs was on coverslips coated with poly-L-ornithine (Sigma-Aldrich) and laminin (Invitrogen). For sequential neuronal and astrocytic differentiation, NPs (2–6.5 × 10^4 cells/cm^2) were cultured without bFGF/EGF. Cells were fixed and stained after 2 d. DAPI-positive cells were scored for TuJ1 staining at 40× magnification in 4 (cerebellar) or 10 (cortical) fields per experimental group (~25–50 cells per field). For astrocyte (GFAP) differentiation, 2% FCS was added to the medium after 3 d, and cells were stained on day 7. Scoring was performed as described for TuJ1 (with 50–100 cells per field). For analysis of ACD, NPs (4.5 × 10^4 cells/cm^2) were cultured 1–7 d in a defined medium (N2-ST: DME/F12/N2, 2% B27 supplement [Invitrogen], 10 ng/ml bFGF, and 1 mM *N*-acetyl-L-cysteine [Sigma-Aldrich]; Qian et al., 2000). For LGN localization, 400 ng/ml nocodazole (Sigma-Aldrich) was added after 17 h, incubated for 6.5 h, and removed 0.5 h before fixation and staining. Frequency of LGN asymmetric distribution was over four independent experiments, including one replicate experiment scored blind. All means and SDs were generated using Excel (Microsoft).

Immunofluorescence

The following antibodies were used: TuJ1 (1:500; Covance), GFAP (1:100; Invitrogen), RC2 and Nestin (1:50; Developmental Studies Hybridoma Bank), LGN (1:100; provided by S. Lanier, Louisiana State University Health Sciences Center, New Orleans, LA; Blumer et al., 2002), α-tubulin (1:500; B512; Sigma-Aldrich), Reelin (1:350; EMD), Brn-1 (1:50; Santa Cruz Biotechnology, Inc.), ABC (1:200; Millipore), NuMa (1:50; Santa Cruz Biotechnology, Inc.), γ-tubulin (1:100; Santa Cruz Biotechnology, Inc.), phosphohistone H3 (1:300; Cell Signaling Technology), cleaved caspase 3 (1:100; Cell Signaling Technology), pan-cadherin (1:100; Santa Cruz Biotechnology, Inc), Vangl2 (1:300; provided by M. Montcouquiol, Institut des Neurosciences de Bordeaux, Bordeaux, France), and secondary antibodies against mouse, goat, or rabbit IgG conjugated to Alexa Fluor 488 (1:100; Invitrogen), Cy3, or Cy5 (1:100; Jackson ImmunoResearch Laboratories). Specificity of LGN antibody (Fig. S3 G) was determined by Western blotting lysates from cerebellar *Lp/Lp* and *Lp/+* NPs, E13.5 whole brain, and from *Xenopus* embryos injected with mRNA as described previously (Brott and Sokol, 2005) with human LGN (hLGN) mRNA (Applied Biosystems) transcribed from pcDNA-hLGN (provided by S. Lanier). For *Xenopus* Stbm (XStbm) functional assays, mRNA (Applied Biosystems) was synthesized from pCS2+CFP-XStbm (provided by M. Mlodzik, Mount Sinai School of Medicine, New York, NY) and pCS2+CFP-XStbmS464N. pCS2+CFP-XStbmS464N was generated by Pfu-directed mutagenesis as described previously (Brott and Sokol, 2005) using the primer 5′-GGCAAAGCAGTGGACGCTGGTTAACGAGGAACCCGTCACCAACG-3′ and confirmed by sequencing. For Western analysis, anti-GFP (JL8; BD) detected XStbm proteins, and anti–β-tubulin (BioGenex) controlled protein loading.

Immunofluorescence experiments of the telencephalic hemispheres were performed at similar points along the anterior posterior axis. Brain tissue from E18.5 *Lp/Lp* (*n* = 4), *Lp/+* (*n* = 2), and +/+ (*n* = 2) mouse embryos was embedded in O.C.T. (Tissue-Tek; Sakura Finetek) and sectioned coronally (10 µm) using a cryostat (Leica). E15.5 *Lp/Lp* (*n* = 3) or +/+ (*n* = 3) were sectioned longitudinally. For asymmetry scoring, E14.5 *Lp/Lp* (*n* = 3) and *Lp/+* (*n* = 3) brains were sectioned coronally (8 µm). Sections were postfixed 15–30 min with paraformaldehyde and 2 min in acetone (or acetone alone for GFAP). Antibody incubations were in PBS-TB (PBS containing 0.2% Triton X-100, 5% donkey or goat serum, and 1% BSA), and washes were in PBS containing 0.2% Triton X-100. For staining NP cultures, cells were fixed in paraformaldehyde (30 min), blocked in 10% goat or donkey serum, and incubated with antibodies in 1.5% serum. Stained samples were mounted in VectaShield (Vector Laboratories) containing DAPI or propidium iodide.

Images were obtained using Axiovision software (Carl Zeiss, Inc.), a microscope (AxioImager; Carl Zeiss, Inc.), and a monochrome X camera (Carl Zeiss, Inc.) at room temperature with fixed samples mounted in VectaShield mounting medium. Basic γ adjustments were performed using either Axiovision software and/or Photoshop (Adobe). Cell images were obtained using 5, 10, 20, 40, and 63× oil objectives with the Apotome attachment (Carl Zeiss, Inc.). Composite images (Fig. S1, A and B) involved overlaying multiple individual fields from a single section in Photoshop. For cleavage plane orientation, anaphase and telophase progenitors were identified in cortical sections costained with γ-tubulin and DAPI, and the angle between the line segregating daughter chromosomes and the ventricular surface was determined using the AxioVision imaging software. For analysis, division angles were grouped into bins at either 10 or 30° increments. Means and standard deviations were generated using Excel. Statistical significance was determined by a standard two-tailed Student's *t* test.

RT-PCR analysis of NPs

RNA was extracted (RNeasy; QIAGEN) from cerebellar (passage 4) or cortical (passage 3) neurospheres for cDNA synthesis with Superscript II (Invitrogen) as recommended by the manufacturer. PCR conditions and primer sequences for *Dlx2*, *BLBP* (*fabp7*), *Mash1*, and *Glast* (slc1a3) were as described previously (Conti et al., 2005). Additional primer sequences were *Nestin* (forward, 5′-AGGAACCAAAAGAGACAGGTG-3′; reverse, 5′-TTCCTCAGATGAGAGGTCAGA-3′) and *GAPDH* (forward, 5′-TTCACCACCATGGAGAAGGC-3′; reverse, 5′-GGCATGGACTGTGGTCATGA-3′).

Online supplemental material

Fig. S1 shows Vangl2 expression, subcellular localization, and functional activity. Fig. S2 shows characterization of cell proliferation and apoptosis in *Lp/Lp* cortices. Fig. S3 shows gene expression and growth properties of *Lp/Lp* NPs. Western blots show specificity of the LGN antibody. Online supplemental material is available at http://www.jcb.org/cgi/content/full/jcb.200807073/DC1.

We thank D. Sassoon and M. Kelley for *Lp/+* mice, S. Lanier and J. Blumer for the LGN antibody and pcDNA-hLGN plasmid, M. Mlodzik for pCS2+CFP-XStbm, and D. Devenport and M. Montcouquiol for the Vangl2 antibody. We also thank J. Hebert and R. Krauss for critical comments on the manuscript.

This study was supported by the National Institutes of Health grants to S.Y. Sokol and the National Sciences and Engineering Research Council of Canada postdoctoral fellowship to B.B. Lake.

Submitted: 14 July 2008
Accepted: 6 March 2009

References

Bellaiche, Y., O. Beaudoin-Massiani, I. Stuttem, and F. Schweisguth. 2004. The planar cell polarity protein Strabismus promotes Pins anterior localization during asymmetric division of sensory organ precursor cells in *Drosophila*. *Development.* 131:469–478.

Betschinger, J., and J.A. Knoblich. 2004. Dare to be different: asymmetric cell division in *Drosophila*, *C. elegans* and vertebrates. *Curr. Biol.* 14:R674–R685.

Blumer, J.B., L.J. Chandler, and S.M. Lanier. 2002. Expression analysis and subcellular distribution of the two G-protein regulators AGS3 and LGN indicate distinct functionality. Localization of LGN to the midbody during cytokinesis. *J. Biol. Chem.* 277:15897–15903.

Bond, J., E. Roberts, G.H. Mochida, D.J. Hampshire, S. Scott, J.M. Askham, K. Springell, M. Mahadevan, Y.J. Crow, A.F. Markham, et al. 2002. ASPM is a major determinant of cerebral cortical size. *Nat. Genet.* 32:316–320.

Brott, B.K., and S.Y. Sokol. 2005. A vertebrate homolog of the cell cycle regulator Dbf4 is an inhibitor of Wnt signaling required for heart development. *Dev. Cell.* 8:703–715.

Chae, T.H., S. Kim, K.E. Marz, P.I. Hanson, and C.A. Walsh. 2004. The hyh mutation uncovers roles for alpha Snap in apical protein localization and control of neural cell fate. *Nat. Genet.* 36:264–270.

Chandran, S., and M.A. Caldwell. 2004. Isolation and characterization of stem cells from the nervous system. *In* Handbook of Stem Cells. Academic Press. 581–591.

Chenn, A., and S.K. McConnell. 1995. Cleavage orientation and the asymmetric inheritance of Notch1 immunoreactivity in mammalian neurogenesis. *Cell.* 82:631–641.

Conti, L., S.M. Pollard, T. Gorba, E. Reitano, M. Toselli, G. Biella, Y. Sun, S. Sanzone, Q.L. Ying, E. Cattaneo, and A. Smith. 2005. Niche-independent symmetrical self-renewal of a mammalian tissue stem cell. *PLoS Biol.* 3:e283.

Du, Q., and I.G. Macara. 2004. Mammalian Pins is a conformational switch that links NuMA to heterotrimeric G proteins. *Cell.* 119:503–516.

Fuja, T.J., P.H. Schwartz, D. Darcy, and P.J. Bryant. 2004. Asymmetric localization of LGN but not AGS3, two homologs of *Drosophila* pins, in dividing human neural progenitor cells. *J. Neurosci. Res.* 75:782–793.

Gho, M., and F. Schweisguth. 1998. Frizzled signalling controls orientation of asymmetric sense organ precursor cell divisions in *Drosophila*. *Nature.* 393:178–181.

Gotz, M., and W.B. Huttner. 2005. The cell biology of neurogenesis. *Nat. Rev. Mol. Cell Biol.* 6:777–788.

Haydar, T.F., E. Ang Jr., and P. Rakic. 2003. Mitotic spindle rotation and mode of cell division in the developing telencephalon. *Proc. Natl. Acad. Sci. USA.* 100:2890–2895.

Jessen, J.R., J. Topczewski, S. Bingham, D.S. Sepich, F. Marlow, A. Chandrasekhar, and L. Solnica-Krezel. 2002. Zebrafish trilobite identifies new roles for Strabismus in gastrulation and neuronal movements. *Nat. Cell Biol.* 4:610–615.

Johe, K.K., T.G. Hazel, T. Muller, M.M. Dugich-Djordjevic, and R.D. McKay. 1996. Single factors direct the differentiation of stem cells from the fetal and adult central nervous system. *Genes Dev.* 10:3129–3140.

Kibar, Z., K.J. Vogan, N. Groulx, M.J. Justice, D.A. Underhill, and P. Gros. 2001. Ltap, a mammalian homolog of *Drosophila* Strabismus/Van Gogh, is altered in the mouse neural tube mutant Loop-tail. *Nat. Genet.* 28:251–255.

Konno, D., G. Shioi, A. Shitamukai, A. Mori, H. Kiyonari, T. Miyata, and F. Matsuzaki. 2008. Neuroepithelial progenitors undergo LGN-dependent planar divisions to maintain self-renewability during mammalian neurogenesis. *Nat. Cell Biol.* 10:93–101.

Kosodo, Y., K. Roper, W. Haubensak, A.M. Marzesco, D. Corbeil, and W.B. Huttner. 2004. Asymmetric distribution of the apical plasma membrane during neurogenic divisions of mammalian neuroepithelial cells. *EMBO J.* 23:2314–2324.

Lee, C.Y., K.J. Robinson, and C.Q. Doe. 2006. Lgl, Pins and aPKC regulate neuroblast self-renewal versus differentiation. *Nature.* 439:594–598.

Montcouquiol, M., R.A. Rachel, P.J. Lanford, N.G. Copeland, N.A. Jenkins, and M.W. Kelley. 2003. Identification of Vangl2 and Scrb1 as planar polarity genes in mammals. *Nature.* 423:173–177.

Noctor, S.C., V. Martinez-Cerdeno, L. Ivic, and A.R. Kriegstein. 2004. Cortical neurons arise in symmetric and asymmetric division zones and migrate through specific phases. *Nat. Neurosci.* 7:136–144.

Qian, X., Q. Shen, S.K. Goderie, W. He, A. Capela, A.A. Davis, and S. Temple. 2000. Timing of CNS cell generation: a programmed sequence of neuron and glial cell production from isolated murine cortical stem cells. *Neuron.* 28:69–80.

Sanada, K., and L.H. Tsai. 2005. G protein betagamma subunits and AGS3 control spindle orientation and asymmetric cell fate of cerebral cortical progenitors. *Cell.* 122:119–131.

Shen, Q., Y. Wang, J.T. Dimos, C.A. Fasano, T.N. Phoenix, I.R. Lemischka, N.B. Ivanova, S. Stifani, E.E. Morrisey, and S. Temple. 2006. The timing of cortical neurogenesis is encoded within lineages of individual progenitor cells. *Nat. Neurosci.* 9:743–751.

Siller, K.H., C. Cabernard, and C.Q. Doe. 2006. The NuMA-related Mud protein binds Pins and regulates spindle orientation in Drosophila neuroblasts. *Nat. Cell Biol.* 8:594–600.

Sokol, S. 2000. A role for Wnts in morpho-genesis and tissue polarity. *Nat. Cell Biol.* 2:E124–E125.

Torban, E., C. Kor, and P. Gros. 2004. Van Gogh-like2 (Strabismus) and its role in planar cell polarity and convergent extension in vertebrates. *Trends Genet.* 20:570–577.

Torban, E., H.J. Wang, A.M. Patenaude, M. Riccomagno, E. Daniels, D. Epstein, and P. Gros. 2007. Tissue, cellular and sub-cellular localization of the Vangl2 protein during embryonic development: effect of the *Lp* mutation. *Gene Expr. Patterns.* 7:346–354.

Tree, D.R., D. Ma, and J.D. Axelrod. 2002. A three-tiered mechanism for regulation of planar cell polarity. *Semin. Cell Dev. Biol.* 13:217–224.

Wolff, T., and G.M. Rubin. 1998. Strabismus, a novel gene that regulates tissue polarity and cell fate decisions in *Drosophila*. *Development.* 125:1149–1159.

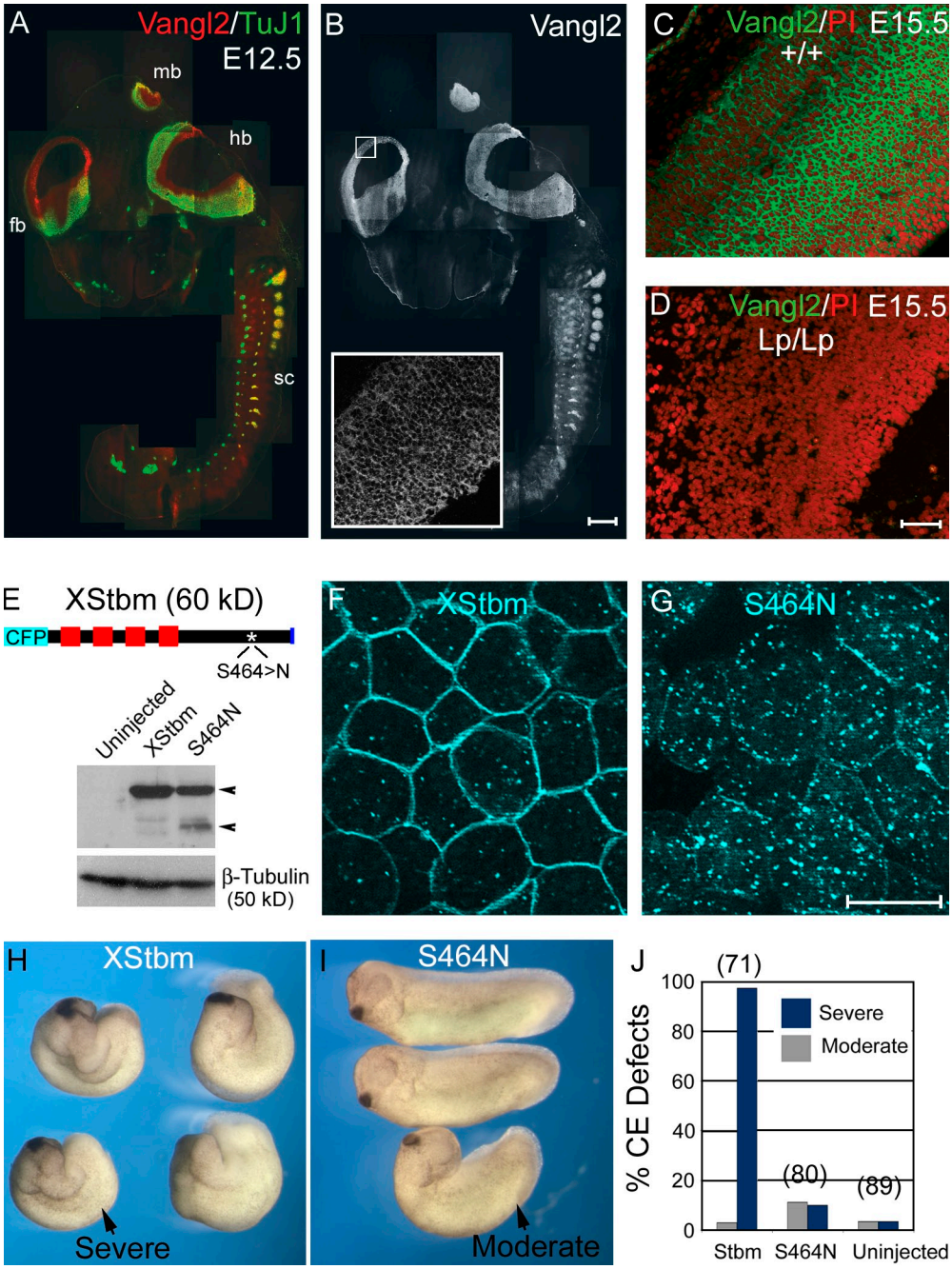

Figure S1. **Vangl2 expression, subcellular localization, and functional activity.** (A–D) Immunolocalization of Vangl2 in the mouse embryonic central nervous system. (A and B) E12.5 wild-type embryos were sectioned longitudinally and stained for Vangl2 and TuJ1. Vangl2 is expressed throughout the forebrain (fb), midbrain (mb), hindbrain (hb), and spinal cord (sc) overlapping neuronal and progenitor layers. The inset in B shows a higher magnification image of Vangl2 staining in the indicated region. The E15.5 *Lp-Lp* cerebral cortex shows significantly reduced staining (D) compared with wild type (C). (E–J) Vangl2/Stbm analysis in *Xenopus* embryos. (E, top) Schematic map of CFP-XStbm. Four transmembrane motifs at the amino terminus and a PDZ-binding motif at the carboxy terminus are indicated. To mimic the *Lp-Lp* mutation, serine at position 464 was converted to an asparagine (S464>N, asterisk). (bottom) In *Xenopus* embryos, XStbmS464N migrates as two distinct bands as compared with wild-type XStbm (arrowheads). β-Tubulin controls for loading. (E–J) Embryos were injected with 1 ng CFP-XStbm and CFP-XStbmS464N mRNAs into the animal pole. In ectodermal cells, CFP-XStbm is mainly at the cell membrane (F), whereas CFP-XStbmS464N is detected in cytoplasmic vesicular structures (G). (H and I) Convergent extension movements in embryos injected with 1 ng CFP-XStbm or CFP-XStbmS464N mRNAs into the dorsal marginal zone (prospective mesoderm). Convergent extension defects were pronounced for XStbm (H) but not for XStbmS464N (I). (J) Summary of results expressed as frequency of affected embryos. Total number of scored embryos is indicated above each bar. CE, convergent extension. Bars: (B) 0.5 mm; (D) 50 µm; (G) 20 µm.

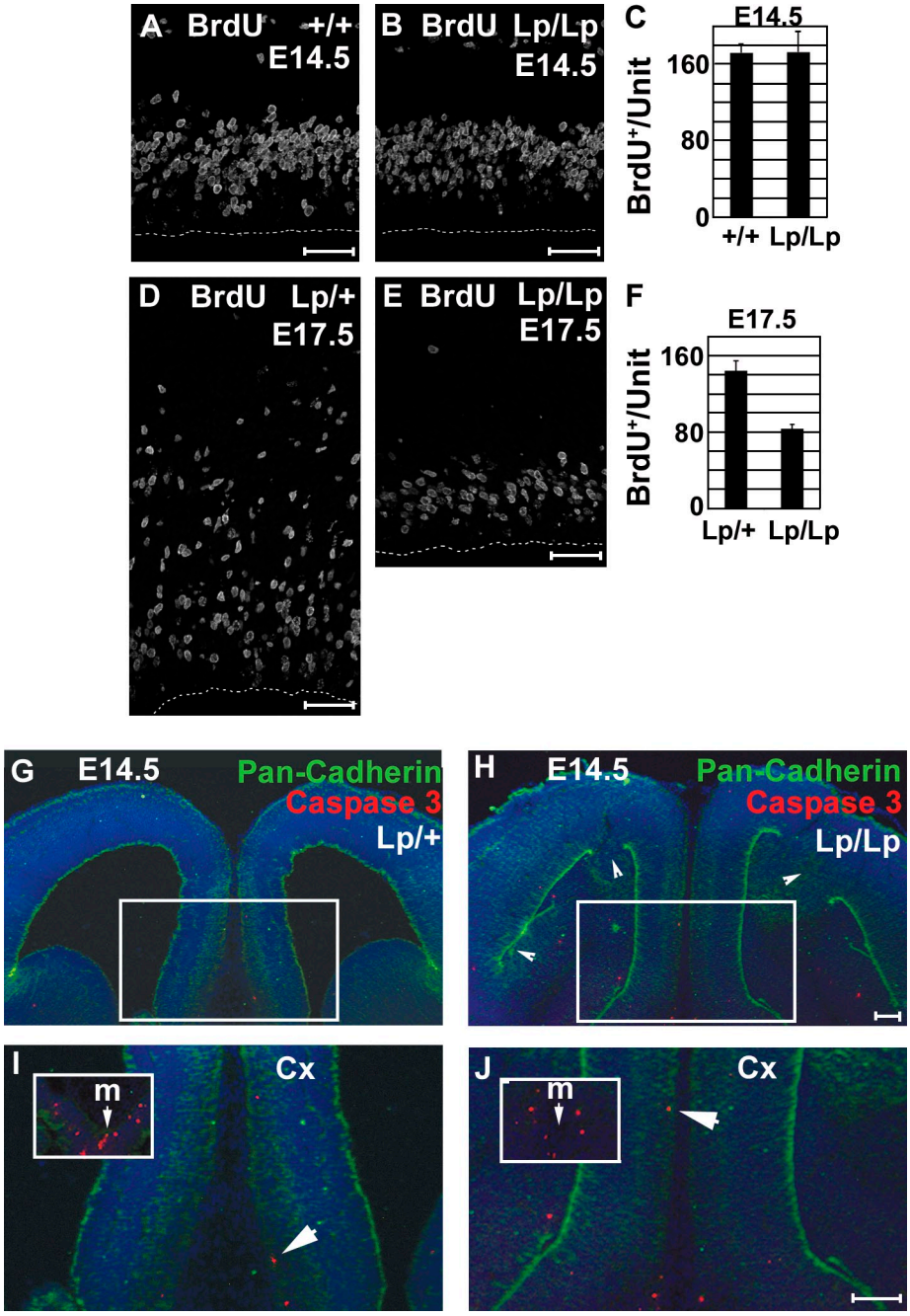

Figure S2. **Characterization of cell proliferation and apoptosis in *Lp/Lp* cortices.** (A–F) BrDU incorporation in *Lp-Lp* VZ NPs. *Lp-Lp* VZ NPs showed normal proliferation during neurogenic stages but reduced proliferation during gliogenic stages of cortical development. BrdU incorporation (1 h pulse labeling) at E14.5 (A–C) and E17.5 (D–F) was measured by the BrdU detection kit (Roche) according to the manufacturer's protocol. At E14.5, both *Lp-Lp* (B) and wild-type (A) cortices showed a similar number of BrdU-positive cells. However, by E17.5, *Lp-Lp* cortices (E) showed significantly fewer BrdU-positive cells than heterozygous littermates (D). Results are presented as average numbers of BrdU-positive cells per field (100 µm of cortex) for three independent cortices ± SD (C and F). (A, B, D, and E) The ventricular surface is indicated by dotted lines. E14.5 brains were sectioned coronally and stained for activated caspase 3 to label apoptotic nuclei (red) and pan-cadherin to label apical membrane (green) and Dapi (blue). *Lp/Lp* cortices (H) resembled that of *Lp/+* littermates (G), with a similar low level of apoptosis restricted primarily to the midline (m; I and J, insets). Boxes in G and H represent areas shown in I and J, respectively. *Lp/Lp* brains exhibited defects of varying penetrance, including disorganized midline/ventral forebrain, occlusion of the lateral ventricles, and areas of abnormal cortical folding (H, arrowheads). Cx, cortex. Arrows indicate apoptotic cells. Error bars indicate SD. Bars: (A, B, D, and E) 50 µm; (H and J) 100 µm.

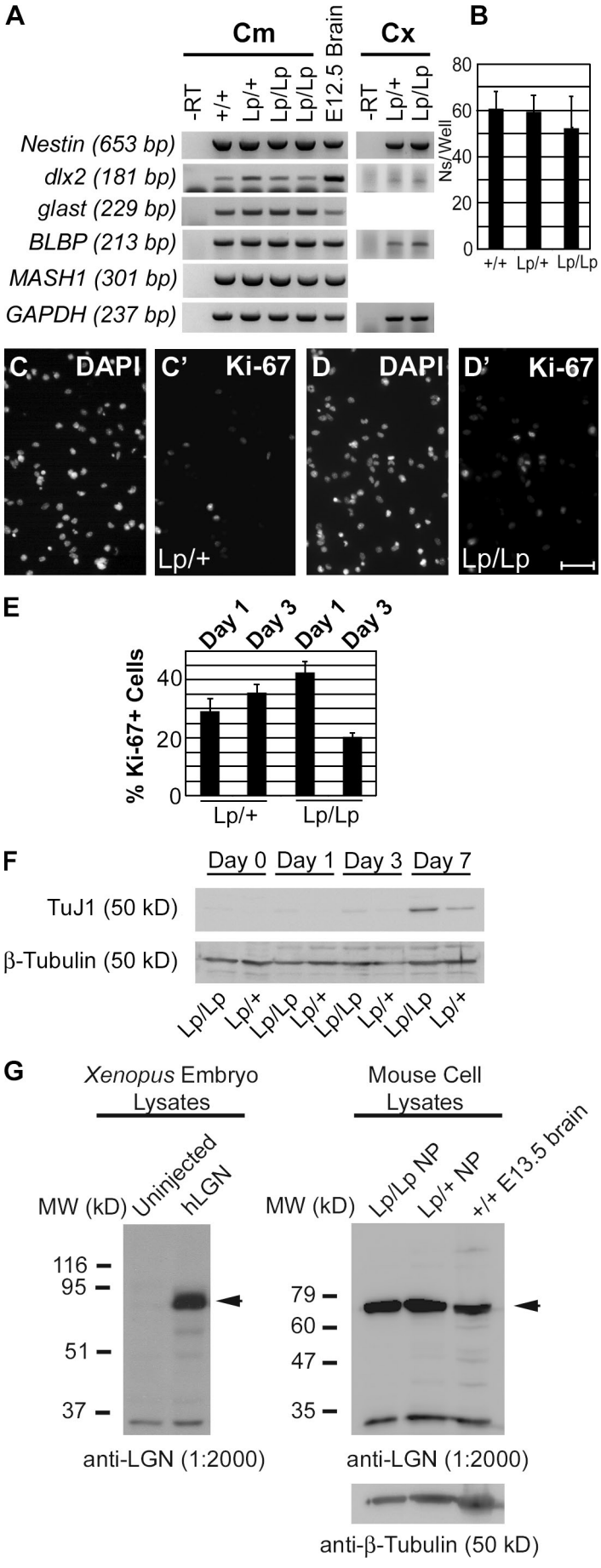

Figure S3. **Gene expression and growth properties of *Lp-Lp* NPs.** (A) RT-PCR analysis of passage 4 neurospheres in comparison with E12.5 wild-type brains. All genotypes show similar levels of the progenitor-specific gene markers *Nestin*, *MASH1*, *Glast*, *BLBP*, and *Dlx2*. *GAPDH* is a control for loading. −RT indicates no reverse transcription; Cm, cerebellum; Cx, cortex. (B–E) Growth of cerebellar *Lp/Lp*, *Lp/+*, and +/+ NPs in culture was compared. (B) Dispersed NP cells (2.5×10^4 cells per well of a 24-well plate) in the presence of bFGF/EGF mitogens formed neurospheres (Ns) after 4 d in culture. The number of neurospheres exceeding 50 µm in diameter is shown for replicate wells. Means ± SD are indicated. (C–E) Number of mitotic nuclei was assessed during *Lp/lp* and *Lp/+* NP differentiation in N2/B27/bFGF media by costaining cells with DAPI and Ki-67 (Novocastra) after 1 d (C–D′) of culture. (E) The frequency of Ki-67–positive cells (relative to total DAPI-positive cells) was significantly reduced in *Lp/Lp* NPs after 3 d of differentiation. Means ± SD are shown for three independent experiments with number of Ki-67–positive cells determined for 10 fields of 50–100 DAPI-positive cells per experiment. (F) Western analysis with anti-TuJ1 antibody reveals premature neuronal differentiation of *Lp/lp* NPs as compared with *Lp/+* NPs that were cultured in the N2/B27/bFGF medium for 0, 1, 3, or 7 d. Note that neuronal differentiation indicated by TuJ1 expression proceeds at a slower rate in this medium as compared with N2 medium alone. Anti–β-tubulin antibody controls loading. (G) Specificity of the LGN antibody. *Xenopus* embryos were injected at the two-cell stage with 1 ng *hLGN* mRNA and cultured until stage 10. Lysates from uninjected and *hLGN* RNA–injected embryos are compared. Mouse cell lysates were obtained from *Lp/Lp* and *Lp/+* neurospheres (cerebellar; passage 5) and E13.5 whole brains. Anti-LGN antibody was used at 1:2,000 dilution. Anti–β-tubulin antibody controls protein loading. Molecular weight (MW) marker positions are indicated. Bar, 50 µm.